Peer reviewed article

In vivo monitoring of magnetically labelled mesenchymal stem cells administered intravascularly in rat acute renal failure

Jun-Hui Sun[a,b], *Gao-Jun Teng*[a], *Zhang-Long Ma*[a], *Sheng-Hong Ju*[a]

[a] Department of Radiology, Zhong-Da Hospital, Southeast University, Jiangsu Key Laboratory of Molecular Imaging and Functional Imaging, Nanjing, China
[b] Department of Hepatobiliary Pancreatic Surgery, the First Affiliated Hospital of Medical College, Zhejiang University, Hangzhou, China

Summary

Questions under study: Many studies have demonstrated that mesenchymal stem cells (MSCs) contribute to the recovery of acute renal failure (ARF). The purpose of the present study was to evaluate *in vivo* tracking of MSCs intravascularly administered in a rat model of ARF for cellular therapy using a 1.5 T MRI system.

Methods: Fe2O3-PLL nanoparticle-labelled and unlabelled MSCs were injected into the abdominal aortas by transcatheterisation of 20 ARF rats, whose renal failure was induced by intramusclar injection of glycerol, while phosphate-buffered saline (PBS) was injected in 20 control rats. Magnetic resonance (MR) images of the kidneys were obtained, before injection of MSCs, after 1 hour, after 1, 2, and 4 days respectively. The MR imaging findings were correlated with the distribution of transplanted MSCs. The kidney injury was histologically evaluated, and the expression of proliferating cell nuclear antigen (PCNA) protein was examined. The Renal function was estimated by quantitative analysis.

Results: In the rat model of ARF the labelled MSCs showed a bilateral loss of signal intensity in the outer zone of the renal cortex on T2*-weighted MR images, which was visible up to 4 days after transplantation. Labelled MSCs were detected in glomerular capillaries by histological examination, the corresponding areas where signal intensity decreased in MR images. Compared to the control group, those ARF rats with MSCs injection had less renal injury, more enhanced tubular cell proliferation and better renal function.

Conclusions: MR imaging visualises those intravascularly administered MSCs *in vivo*, which promoted recovery of ARF.

Key words: magnetic resonance imaging; stem cells; acute renal failure; animal model

Introduction

Acute renal failure (ARF) characterised by a sudden deterioration in renal function may result from one or several factors such as ischaemic or toxic insults etc. Dysfunction or necrosis of renal tubular epithelial cells is the most common pathological change in ARF. Despite technical advances in renal replacement therapy and supportive therapy during the past decades, ARF remains a common intractable clinical problem [1].

Over the past few years, cellular therapy using

Grant: This project was sponsored by the National Nature Science Foundation of China (NSFC30670604) and the Foundation for Excellent Doctoral Dissertations of Southeast University (YBJJ0518).

Abbreviations

ARF	acute renal failure
BUN	blood urea nitrogen
CI	confidence interval
DMEM	dulbecco's modified eagle's medium
Fe2O3	PLL-ferric oxide nanoparticles and coupling with poly-l-lysine
MSCs	mesenchymal stem cells
PBS	phosphate-buffered saline
PCNA	proliferating cell nuclear antigen
SCr	serum creatinine
SD	standard deviation
SNR	signal-to-noise ratio
SPIO	superparamagnetic iron oxide

stem cells has shown great therapeutic promise in the promotion of recovery of organ failure or injury, owing to the cells' innate capability of regenerating damaged tissues and organs [2]. Among the various sources of stem cells, bone marrow-derived mesenchymal stem cells (MSCs) have been the most attractive recently. Bone marrow MSCs have the advantages of easy collection, rapid repopulation *in vitro* and *in vivo*, and are free of societal, ethical and legal disputes, etc. The plasticity of bone marrow MSCs has been widely investigated over the past years. Many studies have demonstrated that MSCs are able to form functional components of other tissues, such as the heart, liver, etc. [2, 3]. Although it is evident that MSCs can differentiate into renal tubular epithelial cells and contribute to the renal repair of acute tubular epithelial injury [4], the renoprotection obtained with MSCs is primarily mediated via complex paracrine actions instead of their differentiation into target cells in an investigation [5]. Therefore, this situation warrants further study to reveal the mechanism of stem cell therapy in ARF.

In order to shed light on the mechanism by which stem cell therapy works, it is essential for the fate of the transplanted cells to be tracked live *in vivo* following their migration, proliferation, differentiation and restoration. In the past few years, MR imaging depicting cells using a cell labelling technique with superparamagnetic iron oxide (SPIO) has become such a valuable technique [6, 7]. MR imaging using SPIO has been confirmed to be practicable for *in vivo* stem cell tracking in spine [8], brain [6], and myocardium [9] or more than one final target organ [10]. With a conventional MRI system, Bos [7] demonstrated *in vivo* that most grafted MSCs distributed into cortical glomeruli in normal kidneys of rats after intravascular injection of the magnetically labelled bone marrow MSCs via the renal artery. Hauger [11] detected intravenously injected MSCs homing in to focal areas of glomerular damage with MR evaluation in a rat model of nephropathy. Clinical ARF characterised by a sudden deterioration in renal function may result from one or several factors such as ischaemic or toxic insults. Since tubular necrosis is the most common pathological lesion in ARF [4] we used a model of ARF induced by intramuscular injection of glycerol in rats, which has similar characteristics to clinical ARF, to evaluate the effects reported in the present study.

The purpose of the present study was to evaluate *in vivo* magnetically labelled bone marrow MSCs injected via transcatherisation into abdominal aortas using a 1.5 T MRI system and to correlate the cellular imaging to their therapeutic effect in rat model of ARF. To the best of our knowledge, this is the first study of *in vivo* MR tracking of the distribution of MSCs following local injection into abdominal aortas in an ARF model induced by intramuscular injection of glycerol.

Methods

Cell culture and identification

This study was approved by our institutional Animal Use and Care Committee. MSCs were generated from the bone marrow of adult Sprague-Dawley rats aged 6 weeks weighing 120–150 g. The bone marrow cells were obtained by flushing the rat femurs with phosphate-buffered saline (PBS). The monocyte layer was selected with density centrifugation and was then re-suspended in low-glucose Dulbecco's modified Eagle's medium (DMEM) (Gibco, Karlsruhe) supplemented with 0.2 mmol/ml L-glutamine, 100 U of penicillin, 100 g/ml streptomycin and 10% foetal bovine serum (Worthington biochemical corporation, Lakewood, NJ). Before being planted in a 25 cm^3 culture flask, the cells were blown into the culture solution, which was adjusted to 1×10^6/ml of the concentration and then grown in standard culture media at 37 °C with 5% CO_2.

The expression of membranous antigen on MSCs was detected by cytofluorimetric analysis with a flow cytometer (Becton Dickinson, San Jose, CA). The primary mouse anti-rat monoclonal antibodies of anti-CD29, anti-CD45 and anti-CD90 (Becton Dickinson, San Jose, CA) were employed. The multipotency of MSCs was confirmed by induction of osteogenic and adipogenic differentiation with specific differentiation media [12]. Osteogenic differentiation was assessed by using von Kossa staining, a way to show the mineralisation, while adipogenic differentiation was visualised by means of oil red O staining of lipid vacuoles in the adipocytes differentiated from MSCs.

Cell labelling and identification of the labelled cells

The Fe_2O_3-PLL nanoparticles were presented by Pro. N Gu (Laboratory of Molecular and Biomolecular Electronics, Southeast University, Nanjing, China). The physico-chemical properties of this SPIO and its efficacy and safety *in vitro* and *in vivo* of labelling on stem cells had been investigated previously in our laboratory [13]. The MSCs grew in 25 cm^3 flasks. The cells growing at $Passage_3$ (P_3) were transferred to the culture media containing Fe_2O_3-PLL for labelling. The concentration of 20 μg/ml iron was used for culture based on our preliminary tests. The MSCs were incubated continuously for 12 h at 37 °C in a 95% air per 5% CO_2 incubator.

The cells were harvested by removing the free Fe_2O_3-PLL washed four times with PBS. For the purpose of Prussian blue staining to identify the cell profile and intracellular iron particles, the cells were continuously incubated for 15 minutes with 2% potassium ferrocyanide in 6% hydrochloric acid, and then counterstained with nuclear fast red for 3 minutes. To measure the iron concentration within the cells, the cell suspension was dissolved in 37% hydrochloric acid and then assayed with a polarised atomic absorption spectrometer (Shengyang Huaguang HG-9602A, Shengyang, China). The measuring process was repeated for three times, and the mean value was adopted.

The distribution of the SPIO particles within the cells was revealed under electron microscopy. The harvested labelled MSCs were fixed at 4 °C in 2.5% buffered

glutaraldehyde for 1 h, followed by 1% osmium tetroxide for 2 h. The samples of these cells were examined with a transmission electron microscope (H600, Hitachi, Japan).

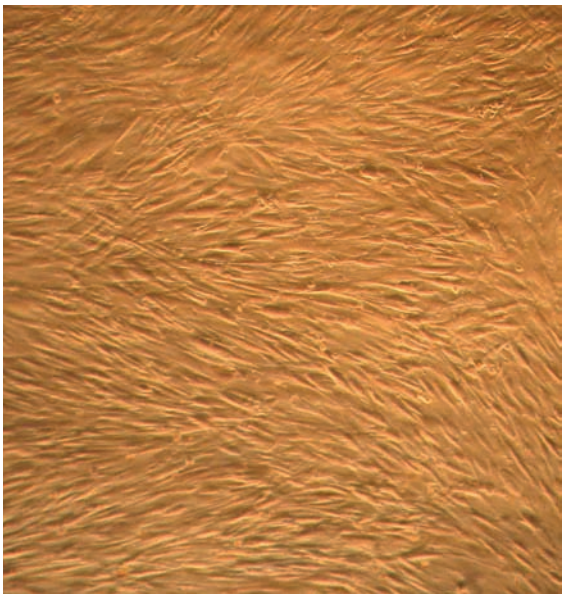

Figure 1

Under an inverse microscopy (×100), Culture bone marrow mesenchymal stem cells (MSCs) (P3) derived from rat appear as uniform fibroblast-like cells with slim bodies.

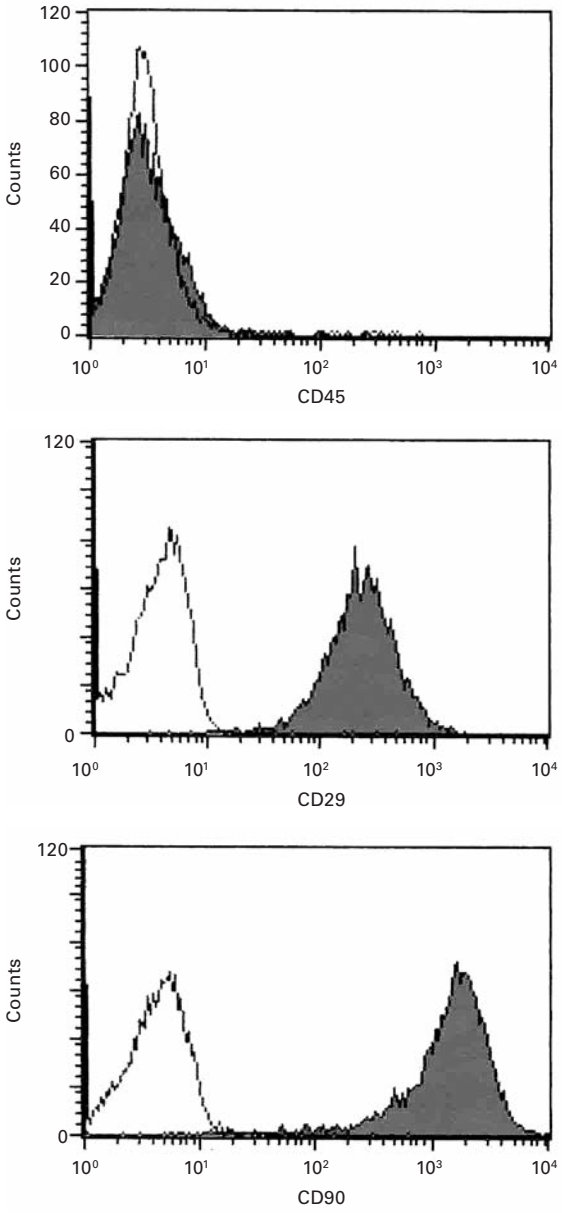

Figure 2

Flow cytometric analysis shows that the mesenchymal stem cells (MSCs) are homogeneous on P3, uniformly positive for the surface proteins of CD29 and CD90, while they are negative for CD45.

Rat model of ARF and MSCs transplantation

A model of ARF was induced by intramuscular injection of glycerol in male SD rats, aged 7 weeks and weighing 200–300 g, based on a standard technique [14]. After anaesthesia with intraperitoneal injection of Pentobarbital (Shanghai Bioengineering Co., Shanghai, China) at 40 mg/kg, 50% glycerol (Shanghai Bioengineering Co., Shanghai, China) in normal sodium at dose of 8 ml/kg was injected into both posterior thigh muscles of the rats. Before glycerol injection, the animals were allowed to eat freely, but deprived of drinking water for 17 h. After successful induction of ARF 2 days after glycerol injection, the rats were randomly divided into three groups: group A (transplanted with labelled cells, n = 20), group B (transplanted with unlabelled cells, n = 20) and group C (control group, PBS injected only, n = 20). All the rats survived after the glycerol injection before the ending of this study.

Labelled and unlabelled MSCs were trypsinised, centrifuged, and washed with PBS, which were counted in a microcytometer chamber and resuspended in DMEM. A modified catheter from PE-50 line was inserted into the the suprarenal aorta via the right femoral or iliac artery exposed surgically. One ml of DMEM containing 2×10^6 labelled or unlabelled cells, or 1 ml PBS was injected into the abdominal aorta via the catheter.

MR imaging

MR images of the kidneys of the recipients were obtained before injection of MSCs, and 1 h, 1, 2, and 4 days post transplantation, respectively. MR imaging was performed with a 1.5 T MRI system (Eclipse, Philips Medical Systems) using a 12.7 cm receiver with surface coil only. The MR imaging sequence was T2*-weighted gradient-echo (620/15.7; flip angle, 35^0) sequence. Images were taken with a matrix size of 256 × 256, section thickness of 2.5 mm, and field of view of 8 × 6 cm, two measurements were acquired.

Mean signal intensities at four interesting regions in each kidney were evaluated by one of the authors (S.H.J.), an experienced radiologist practicing MR image analysis for 14 years, who was blinded to the transplanting procedure. Signal-to-noise ratio (SNR) of the outer zone of the renal cortex on T2*-weighted MR imaging calculated by dividing signal intensity by the background noise [10, 15] was obtained before and 1 hour, 1, 2, 4 days after transplantation, respectively.

Evaluation of renal function

Serum creatinine (SCr) and blood urea nitrogen (BUN) in blood samples collected from the tail vein of the rats were measured by an autoanalyser (7150, Hitachi, Japan) immediately after the MRI examinations before and 1, 2, 4 days post transplantation, respectively.

Histopathological and immunohistochemical analysis

Five rats selected randomly in each group were euthanised at 1h, 1, 2 and 4 days, respectively post cell transplantation following the MR examination. The histological examinations of the kidneys were performed immediately after sacrifice. After perfusion and fixation in 4% buffered paraformaldehyde for 24 h at least, 5 μm-thick sections were cut and stained with haematoxylin/eosin (H&E Stain).

The degree of tubular injury was scored by a previously reported approach [5, 16] in random (using a simple random sampling table) cortical fields using a graduated grid with 25 squares with a ×20 lens. One hundred intersections between tubular profiles and the grid were examined in each kidney. A score for each tubular cross

section per intersection was assigned as follows: 0 = normal histology; 1 = tubular cell swelling, loss of brush border, nuclear condensation, up to one-third of tubular cross section showing nuclear loss; 2 = same as for score 1, except for greater than one-third and less than two-thirds of nuclear loss per tubular cross section; and 3 = greater than two-thirds of tubular cross section shows nuclear loss. The total score for each kidney was calculated by the addition of all 100 scores (the higher the score, the more serious the tubular injury). The total injury score for each kidney was calculated by one of the authors (Z.L.M.) with 10 years' experience of histopathological analysis who was blinded to the transplanting procedure.

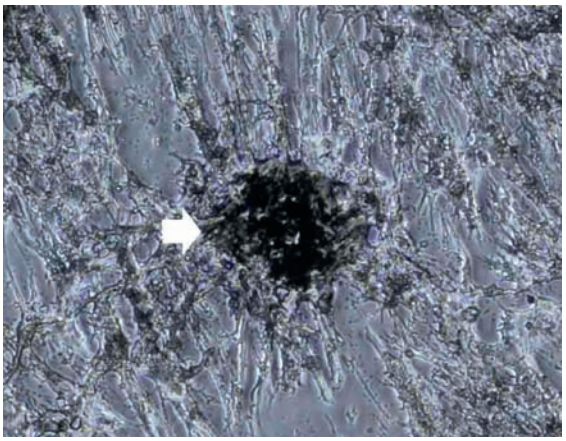

Figure 3

Mesenchymal stem cells (MSCs) (P3) exhibit nodular aggregation on the von Kossa staining mineral (arrows) after osteogenic induction.

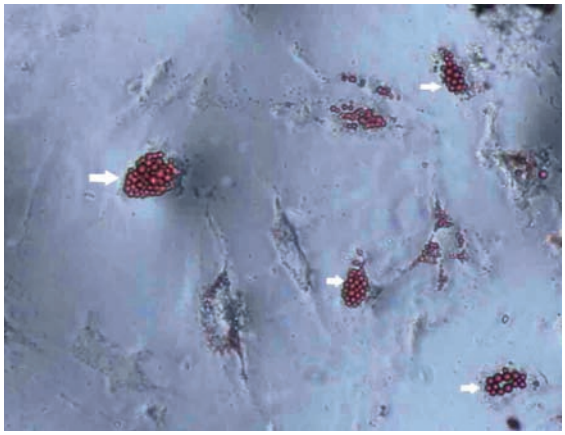

Figure 4

Intracytoplastic lipid vesicles (arrows) are observed on the oil red O staining after adipogenic induction.

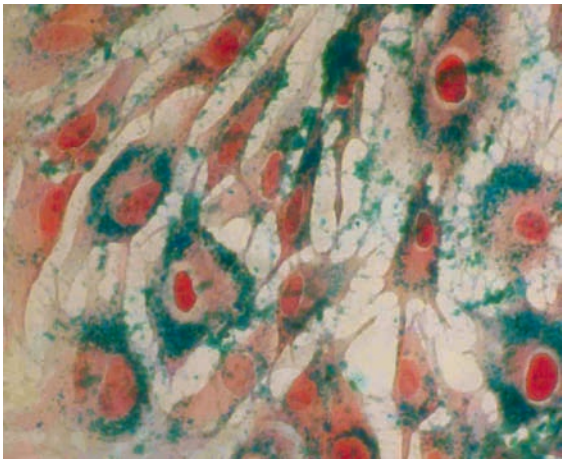

Figure 5

Intracytoplasmic blue particles in most mesenchymal stem cells (MSCs) (P3) incubated with ferric oxide nanoparticles and coupling with poly-l-lysine (Fe2O3-PLL) are clearly visible with Prussian blue staining (×400).

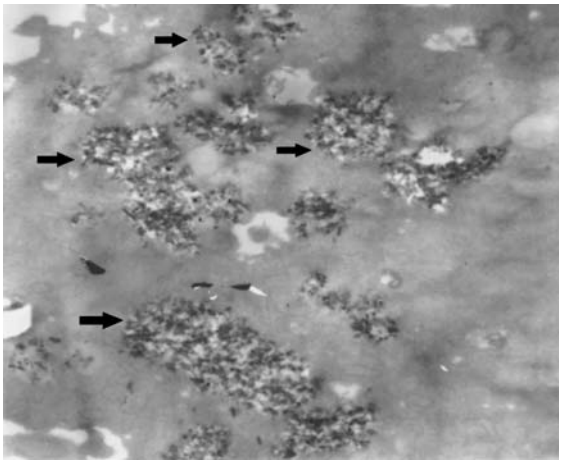

Figure 6

The endosomal vesicles (arrows) containing superparamagnetic iron oxide (SPIO) particles appear inside the mesenchymal stem cells (MSCs) (P3) in the transmission electron micrograph (original amplification: ×15 000).

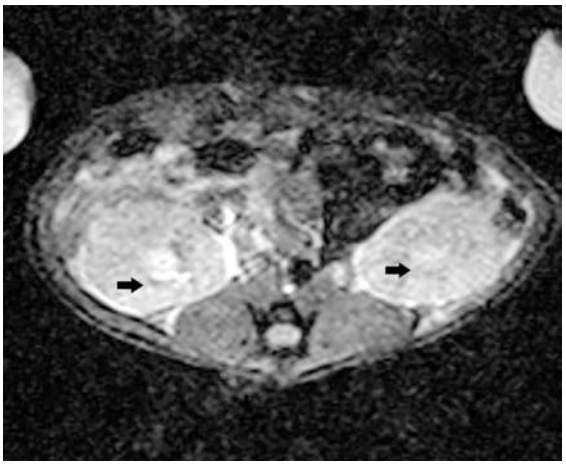

Figure 7

Transverse T2*-weighted MR image of the rat kidney obtained before mesenchymal stem cells (MSCs) injection shows mild signal intensity decrease around the renal pelvis (arrows).

Figure 8

Coronal T2*-weighted MR image of the rat kidney obtained 1 h after injection with the labelled mesenchymal stem cells (MSCs) shows a signal intensity decrease (arrows) in the outer zone of the renal cortex.

Table 1

Renal function parameters of the rats in 3 groups at different time points before and after mesenchymal stem cells (MSCs) or phosphate-buffered saline (PBS) administration.

Groups	A	B	C	95% confidence intervals (CI) C-AB
Serum creatinine (SCr) (μmol/L)				
Before injection (n = 5)	519 (55)	490 (46)	510 (57)	–114–126
1 day post injection (n = 5)	499 (49)	437 (38)	483 (17)	–94–125
2 days post injection (n = 5)	194 (30)	211 (38)	331 (52)*	39–219
4 days post injection (n = 5)	91 (14)	85 (22)	154 (15)*	29–103
blood urea nitrogen (BUN) (mmol/L)				
Before injection (n = 5)	49 (6)	55 (6)	53 (9)	–17–18
1 day post injection (n = 5)	46 (5)	49 (5)	47 (6)	–13–11
2 days post injection (n = 5)	23 (4)	21 (4)	36 (4)*	6–24
4 days post injection (n = 5)	9 (2)	10 (3)	17 (2)*	3–13

Note. – Values are expressed as mean (SD).
Significant difference as compared with group A or B (P <0.05, two-tailed).

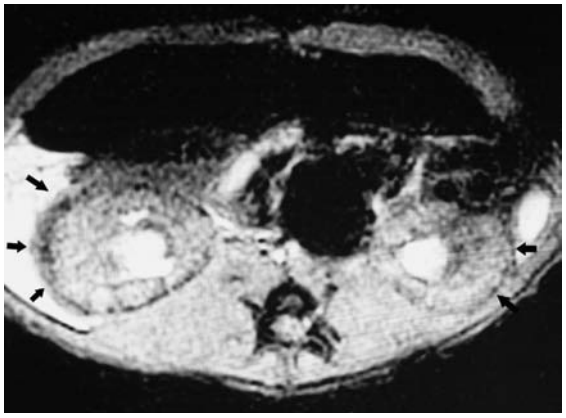

Figure 9

Signal intensity loss in the outer zone of the renal cortex (arrows) is detected on transverse T2*-weighted MR image of the kidney obtained 1 h after injection with the labelled mesenchymal stem cells (MSCs).

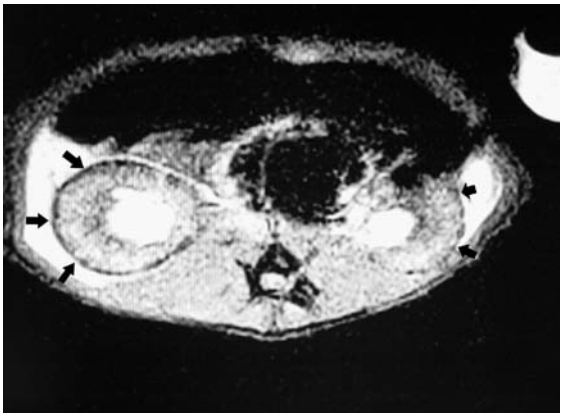

Figure 10

On the 4th day after labelled *mesenchymal stem cell (MSC)* transplantation, the signal intensity decrease (arrows) is still visible on the transverse T2*-weighted MR image.

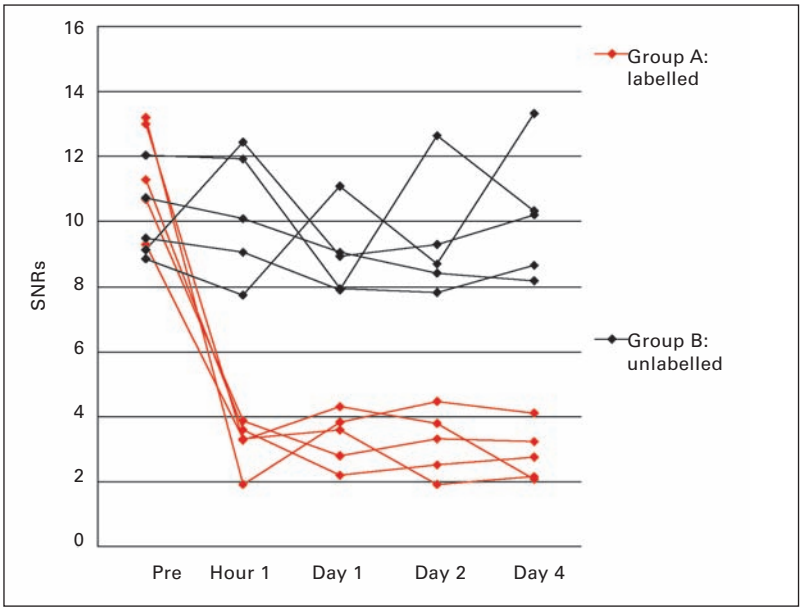

Figure 11

Quantitative measurement of signal-to-noise ratio (SNR)s of outer zone of rats renal cortex on T2*WI at different time points before and after administration of labelled mesenchymal stem cells (MSCs) (group A, red line) and unlabelled MSCs (group B, black line): one line for each rat. In group A, there is significant SNR decrease of renal cortex 1 hour, 1, 2, 4 days after labelled MSCs transplantation, while there is no significant SNR difference among different time points in group B.

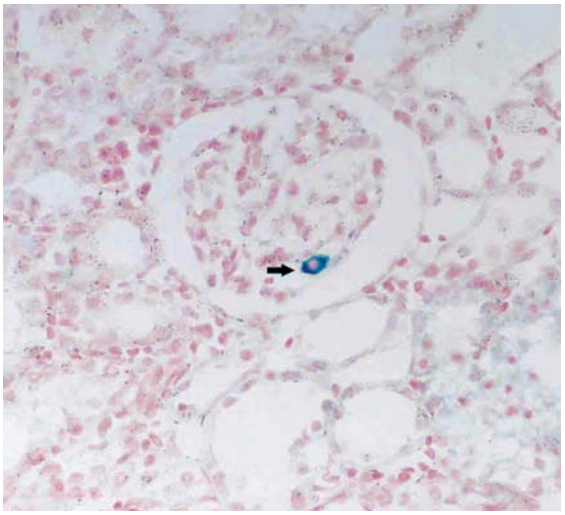

Figure 12

Most cells positive for Prussian blue staining (arrow) are located in the glomeruli in outer zone of renal cortex in the kidneys of group A (transplanted with labelled cells), which corresponds to the signal intensity loss observed in MR image. (Prussian blue staining, ×100)

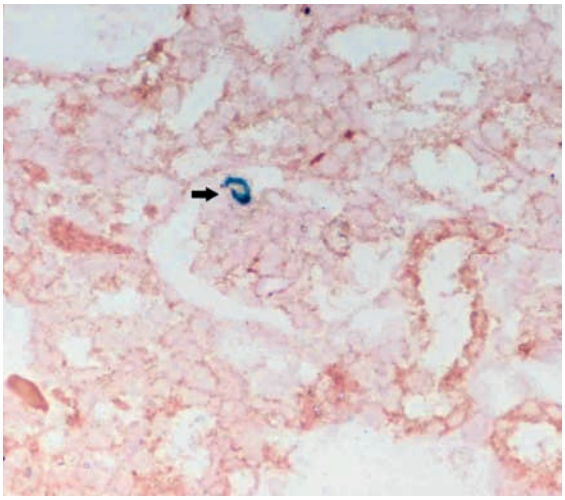

Figure 13

Dual stainings of CD68 and Prussian blue in the renal tissues of group A (transplanted with labelled cells) show negative CD68 in Prussian blue stain-positive cells (arrow, ×100).

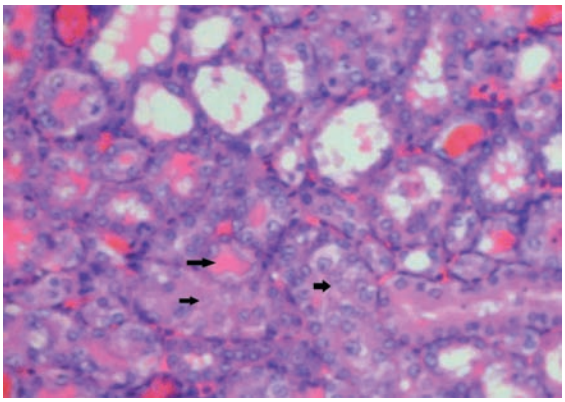

Figure 14

Histological sections of the kidney in group C (control group, phosphate-buffered saline injected only) at 4 days after injection of phosphate-buffered saline showing serious tubular necrosis and intra-tubular casts. (arrows, Haematoxylin & eosin-stained, ×400).

Prussian blue staining was performed to assess the localisation of the iron-loaded MSCs. Dual staining of Prussian blue and CD68 (immunohistochemistry) were used for identifying infiltrating macrophages that might be iron-positive. Immunohistochemistry assay of CD68 was performed on paraffin sections, stained with a mouse anti-rat monoclonal antibody of anti-CD68 (Biolegend, San Diego, CA).

Proliferative cell nuclear antigen (PCNA) was also determined on paraffin sections using a rabbit polyclonal antibody (Biolegend, San Diego, CA). The PCNA positive nuclei in the renal medulla and cortex were quantified under a light microscope at a magnification of 400 times and were expressed as mean values on day 4 post MSC administration based on the examination of 50 fields in each experimental animal by an author (Z.L.M.) who was blinded to the treatment of each rat according to a previously reported method [17].

Statistical analysis

Statistical analyses were carried out with the SPSS software (SPSS for Windows, version 11.0, 2001; SPSS, Chicago, Ill). Values were expressed as mean (standard deviation, SD). A consistent notation was adopted when reporting means and confidence intervals (CI). Differences of the means among the groups were analysed using one-way analysis of variance (ANOVA) followed by Dunnett's or LSD test. A p value (two-tailed) of less than 0.05 was considered as statistically significantly different.

Results

Characterisation of MSCs

When they were passed to P_3, the purified MSCs remained in the pattern of uniform fibroblast-like cells (fig. 1). These MSCs, as a single phenotypic population, were able to be further cultured and passed, and proliferated rapidly. The homogeneity of the cells reached 99%. The surface proteins, the characteristics of MSCs, such as CD29 and CD90, were uniformly positive, while CD45 as an indicative marker for haematopoietic lineage was negative (fig. 2). MSCs showed positive with von Kossa staining for the mineralisation nodules after osteogenic induction (fig. 3). Intracytoplastic lipid vesicles were demonstrated by oil red O staining after adipogenic induction (fig. 4). The cells used in the subsequent experiments were those characterised by confirmation of their multipotency and the specific markers of the surface proteins.

In vitro cell labelling

Blue particles were clearly shown within almost every labelled cell on the Prussian staining slides (fig. 5), however they were not found in the unlabelled cells. The iron quantification per cell measured by atomic absorption spectrometer was 12.6 (2.6) picograms. The SPIO particles located in the endosomal vesicles of the cells were confirmed by transmission electron microscopy (fig. 6).

In vivo MR imaging of the labelled MSCs

Before injection of the labelled cells into the suprarenal aorta, a mild signal intensity loss was shown around the renal pelvis on T2*-weighted MR images (fig. 7). In group A, signal intensity loss in the outer zone of the renal cortex was demonstrated on T2*-weighted MR images 1 h after transplantation (fig. 8, 9). Since then, the remarkable visual regional signal intensity loss lasted for 4 days following the transplantation (fig. 10). Signal intensity loss was not detected in group B. Before and 1 hour, 1, 2 and 4 days after injection, the outer zone of renal cortex SNRs were 11.5 (1.5), 3.2 (0.8), 3.3 (0.8), 3.0 (0.9), 2.9 (0.8) respectively for group A, and 10.1 (1.2), 10.3 (1.8), 9.0 (1.2), 9.4 (1.7), 10.1 (1.8) for group B. Injection of labelled cells caused a significant SNR decline in renal cortex for group A at 1 hour, 1, 2, and 4 days after injection compared to group A rats before transplantation or group B control rats (ANOVA, P <0.001; Dunnett's test, P <0.001, respectively, 95% CI: 6.4–8.7). For the control group B, there was no statistically significant difference in SNR at each time point compared to pretransplantation (ANOVA, P = 0.799, 95% CI: –3.1–1.9) (fig. 11).

Renal function of rats with ARF after MSC transplantation

Before the experiment of the cell transplantation, ARF model of the rats had been confirmed by a significant increase of SCr and BUN concentrations 2 days after glycerol administration, which reached the peak concentrations on the 2nd day following glycerol injection.

The measurements of renal function were shown by SCr and BUN changes of group A, B and C at different time points after transplantation (table). The Rats in group A and B had a significantly better renal function at 2 and 4 days, respectively post MSC administration than that in group C, as demonstrated by SCr (ANOVA, P = 0.012; LSD test, P = 0.006, P = 0.011, respectively, at 2 days; ANOVA, P = 0.005; LSD test, P = 0.004, P = 0.003, respectively, at 4 days) and BUN levels (ANOVA, P = 0.006; LSD test, P = 0.006, P = 0.003, respectively, at 2 days; ANOVA, P = 0.011; LSD test, P = 0.006, P = 0.009, respectively, at 4 days), while there were no significant differences of SCr (LSD test, P = 0.637, P = 0.705, respectively, at 2 days and 4 days) and BUN (LSD test, P = 0.598 P = 0.771, respectively, at 2 days and 4 days) levels between group A and B. There were no significant differences of SCr (ANOVA, P = 0.800) and BUN (ANOVA, P = 0.572) levels among three groups before MSC or PBS injection. There also were no significant differences of SCr (ANOVA, P = 0.210) and BUN (ANOVA, P = 0.699) levels among three groups on day 1 after MSC or PBS injection.

Histological analysis

In group A, positive Prussian blue staining, the characteristic phenotype of the iron-labelled MSCs, was revealed in the glomerular capillaries in the outer zone of the renal cortex, which corresponded well with the signal extinction observed on MRI, however it was not detected in the rats injected with unlabelled cells (fig. 12). None of the iron-loaded cells were positive for CD68 in the dual staining of CD68 and Prussian blue in kidney tissues (fig. 13), which was considered as a protein characteristic of macrophages. Few iron-labelled MSCs were found in the interstitial tissues of the kidney, and no iron-labelled MSCs were detected in the renal tubules.

Tubular epithelial injury was evident on day 2 post glycerol injection. The morphological changes observed in animals with glycerol-treated ARF included tubular hyaline cast formation and widespread necrosis of tubular epithelial cells (fig. 14). The tubular lesions of the rats in group A and B were less severe on the 4th day after MSC injection than in group C. The renal injury scores of the three groups were 103(27), 110(30), 201(30), respectively. The scores of group C were significantly higher than in group A and B (ANOVA, P <0.001; LSD test, P <0.0001, P <0.0001, respectively, 95%CI C-AB: 57–133), while there was no significant difference in the renal injury scores between group A and B (ANOVA, P <0.001; LSD test, p = 0.660, 95% CI C-AB: –42–27).

The numbers of PCNA positive tubular cells detected at day 4 after MSC or PBS injection in group A, B and C were 33(6), 34(6), 16(4)/HPF ×400, respectively. The proliferation of tubular cells positive for PCNA staining was significantly higher in group A and B compared to group C (ANOVA, P <0.001; LSD test, P <0.0001, P <0.0001, respectively, 95% CI C-AB: 15–20), While there was no significantly difference between group A and B (ANOVA, P <0.001; LSD test, p = 0.76, 95% CI C-AB: –2–3).

Discussion

ARF, which is associated with high morbidity and mortality, occurs frequently in hospitalised patients [18]. A series of circumstances, including primary renal diseases, impaired renal perfusion, hypovolaemia, sepsis, vascular occlusion and drug toxicity etc, leading to irreversible injury of the glomerular and tubular cells, culminates in acute renal failure [1]. Stem cell transplantation in kidneys was investigated in the past few years due to its potential capability for repairing various diseased organs and tissues [2, 3]. Successful differentiation into glomerular mesangial cells from the bone marrow-derived stem cells in rats has been reported [19]. Moreover, it has been demonstrated by several groups that transplantation of MSCs improved renal function, and MSCs reconstituted the renal epithelium by transdifferentiation [20]. However, the mechanisms by which renoprotection arises following MSC transplantation are disputed. Togel and colleagues [5, 21] indicated that the effectiveness of renoprotection obtained with MSCs for ARF induced by ischaemic injury was likely to be mediated primarily via complex paracrine actions instead of the MSCs' differentiation into target cells, because there was no evidence of transdifferentiation of the grafted MSCs into renal cells up to 3 days after implantation. The mechanism of glycerol induced ARF, which had been used in the present research, is different from the ischaemic induction of ARF mentioned above. The intramuscular administration of hypertonic glycerol induces rhabdomyolysis with a lot of myoglobin being released into the circulation with three major pathophysiological effects: renal vasoconstriction, direct cytotoxicity, and cast formation. Hypovolaemia and

metabolic acidosis facilitate tubular precipitation of myoglobin, besides causing tubular obstruction, may contribute to tubular epithelial cell injury through a probable haem-iron-mediated lipid peroxidation mechanism. This latter process further compromises the tubular fluid flow dynamics, and interferes with the complete clearance of tubular haem proteins, thus initiating the vicious cycle ultimately leading to ARF [14]. These are similar characteristics to clinical ARF.

During recent years, several noninvasive *in vivo* tracking molecular imaging techniques including nuclear medicine, optical imaging and MR imaging have been developed [22–24]. MR technique holds promising advantages due to its properties of wide imaging window, high temporal and spatial resolution, and good contrast but without ionic radiation.

Recently, great progress in cell labelling techniques using SPIO has been achieved [13, 25]. SPIO particles nanometric in size have several advantages described previously, which include properties of biological degradation, ease of metabolism and integration into the serum Fe pool to form haemoglobin or enter other metabolic processes [26], and have strong penetrating capability which makes it possible to cause signal change in MR imaging at a super-low tracer concentration. Our previous study showed that the SPIO particles we used in this study have a high labelling rate and impact little influence on cells' biological properties [13]. Several groups have demonstrated the feasibility of *in vivo* tracking of transplanted stem cells by magnetically labelling them with SPIO particles [6–9]. Hauger [11] detected intravenously injected MSCs homing to focal areas of damaged glomeruli using 4.7-T Micro-MR system. Although imaging with micro-MR imaging systems may have more sensitive and higher spatial resolution, Bos [7] demonstrated that SPIO labelled MSCs in normal kidneys of rats injected intravascularly via renal artery can be followed using a conventional MRI system.

In the literature two approaches to *in vivo* MR tracking for renal cell transplantation have been reported [7, 11]: stem cells were injected into kidneys via either the renal arterial or intravenous injection. Obviously, intravenous injection of the cells is associated with the problem of a small number of cells homing to the targeted organ as well as the complicated mechanism of cell homing. Furthermore, the migration speed of the grafted cells is slow. So this approach might not be appropriate for cell therapy for diffuse acute organ diseases such as ARF. Renal arterial administration of cells in contrast, has the advantage of delivering a large amount of cells directly to the organ and distributing them throughout the whole kidney with a single injection. However, single renal arterial injection can only delivery the cells into one kidney directly. Administration of cells into the abdominal aorta might distribute the cells throughout both kidneys with a single perfusion. Therefore, we developed a new approach of injecting MSCs into the abdominal aorta above the renal arteries. It is expected that this new technique might replace the two approaches mentioned above. The results of this study indicate that this goal seems to have been achieved. The MR imaging showed that the MSCs injected into the suprarenal aorta distributed predominantly into the glomeruli in the outer zone of the cortex of ARF kidneys. The distribution of MSCs lasted for 4 days after transplantation, which might be related to mechanical trapping in the glomerular tuft or specific homing. The results regarding renal function and histopathology in this study were similar to those of the previous experiments in the literature [4, 21] although the different approach of transplantation and a different animal model were used. Herrera demonstrated that MSCs injected intravenously homed to the kidney of mice with glycerol-induced ARF and promoted the recovery of renal damage [4]. The MSCs were found to be located in the kidney cortex after injection into the thoracic aorta of rats with ischaemia/reperfusion ARF for 72 h, and the infusion of MSCs enhanced recovery of renal injury [21]. No Prussian blue staining-positive tubules and vascular endothelial cells were demonstrated in 4 days after cell injection, which suggests that the transdifferentiation process from the grafted MSCs into the renal tubular epithelial cells was uncertain up to 4 days post cell transplantation. However, the animals administered with MSCs had less severe tubular injury, more enhanced tubular proliferation and regeneration indicated by increased PCNA expression, and better renal function compared to those in the control group. Therefore, we are assume that the renoprotective effect of MSC transplantation during the early stages of ARF induced by nephrotoxic injury is not mainly mediated by transdifferentiation mechanism but via complex paracrine actions. The finding that no significant differences of renal function and histological findings between the groups with labelled or unlabelled MSCs indicate that SPIO labelling has little influence on the cells' biological properties *in vivo*.

There were several limitations in this study. Firstly, the number of animals used in this experiment was small, which decreased the statistical power of our results although it was sufficiently large to obtain the main conclusion. Secondly, the long-term fate of the MSCs in the rat model of ARF was not observed due to the short-term follow-up of 4 days. Thirdly, the MR imaging, for its limited spatial resolution, failed to reveal the delicate anatomical structures of the kidney, which might reflect the cellular therapeutic outcomes, and therefore it was impossible to correlate the MRI findings with the histopathological findings of the renal injury.

In conclusion, this study demonstrates that

MSCs intravascularly injected via abdominal aorta mainly distribute within the renal glomerular capillaries. The effectiveness of renoprotection is confirmed in a nephrotoxic ARF rat model. However, our study suggests that the mechanism of this renoprotective effect may not mainly depend on the transdifferentiation from the transplanted stem cells into the target renal cells. Our results indicate that MSCs' vitality is not influenced by SPIO labelling *in vivo*.

There is no doubt that cellular therapy has promising potential in renal disease, especially for end-stage renal failure, ARF or chronic acute failure, etc. Apparently, this *in vivo* monitoring technique is useful for future investigation of cell therapy in the kidney, especially in depicting *in vivo* cells administrated by various approaches into kidneys and for studying the renoprotective mechanisms of cell therapy.

The authors thank Dr. Li Li for her efforts in English language revision of the manuscript.

Correspondence:
Gao-Jun Teng, MD
Department of Radiology
Zhong-Da Hospital, Southeast University
87 Ding Jia Qiao Road
Nanjing 210009, China
E-Mail: gjteng@vip.sina.com

References

1 Ympa YP, Sakr Y, Reinhart K, Vincent JL. Has mortality from acute renal failure decreased? A systematic review of the literature. Am J Med. 2005;118:827–32.
2 Dai W, Hale SL, Martin BJ, Kuang JQ, Dow JS, Wold LE, et al. Allogeneic mesenchymal stem cell transplantation in postinfarcted rat myocardium: short- and long-term effects. Circulation. 2005;112:214–23.
3 Sato Y, Araki H, Kato J, Nakamura K, Kawano Y, Kobune M, et al. Human mesenchymal stem cells xenografted directly to rat liver are differentiated into human hepatocytes without fusion. Blood. 2005;106:756–63.
4 Herrera MB, Bussolati B, Bruno S, Fonsato V, Romanazzi GM, Camussi G. Mesenchymal stem cells contribute to the renal repair of acute tubular epithelial injury. Int J Mol Med. 2004;14: 1035–41.
5 Togel F, Hu Z, Weiss K, Isaac J, Lange C, Westenfelder C. Administered mesenchymal stem cells protect against ischemic acute renal failure through differentiation-independent mechanisms. Am J Physiol Renal Physiol. 2005;289:F31–42.
6 Hoehn M, Kustermann E, Blunk J, Wiedermann D, Trapp T, Wecker S, et al. Monitoring of implanted stem cell migration in vivo: a highly resolved in vivo magnetic resonance imaging investigation of experimental stroke in rat. Proc Natl Acad Sci. USA 2002;99:16267–72.
7 Bos C, Delmas Y, Desmouliere A, Solanilla A, Hauger O, Grosset C, et al. In vivo MR imaging of intravascularly injected magnetically labelled mesenchymal stem cells in rat kidney and liver. Radiology. 2004;233:781–9.
8 Bulte JW, Zhang S, van Gelderen P, Herynek V, Jordan EK, Duncan ID, et al. Neuro transplantation of magnetically labelled oligodendrocyte progenitors: magnetic resonance tracking of cell migration and myelination. Proc Natl Acad Sci. U S A 1999;96:15256–61.
9 Kraitchman DL, Heldman AW, Atalar E, Amado LC, Martin BJ, Pittenger MF, et al. In vivo magnetic resonance imaging of mesenchymal stem cells in myocardial infarction. Circulation. 2003;107:2290–3.
10 Daldrup-Link HE, Rudelius M, Piontek G, Metz S, Brauer R, Debus G, et al. Migration of iron oxide-labelled human hematopoietic progenitor cells in a mouse model: in vivo monitoring with 1.5-T MR imaging equipment. Radiology. 2005; 234:197–205.
11 Hauger O, Frost EE, van Heeswijk R, Deminiere C, Xue R, Delmas Y, et al. MR evaluation of the glomerular homing of magnetically labelled mesenchymal stem cells in a rat model of nephropathy. Radiology. 2006;238:200–10.
12 Pittenger MF, Mackay AM, Beck SC, Jaiswal RK, Douglas R, Mosca JD, et al. Multilineage potential of adult human mesenchymal stem cells. Science. 1999;284:143–7.
13 Ju SH, Teng GJ, Zhang Y, Ma M, Chen F, Ni YC. In vitro labelling and MR imaging of mesenchymal stem cells from human umbilical cord blood. Magn Reson Imaging. 2006;24: 611–7.
14 Zager RA, Burkhart KM, Conrad DS and Gmur DJ. Iron, heme oxygenase, and glutathione: effects on myohemoglobinuric proximal tubular injury. Kidney Int. 1995;48:1624–34.
15 Wolff S, Balaban R. Assessing contrast on MR images. Radiology. 1997;202:25–9.
16 Chatterjee PK, Brown PA, Cuzzocrea S, Zacharowski K, Stewart KN, Mota-Filipe H, et al. Calpain inhibitor-1 reduces renal ischemia/reperfusion injury in the rat. Kidney Int. 2001;59: 2073–83.
17 Zhou H, Kato A, Yasuda H, Miyaji T, Fujigaki Y, Yamamoto T, et al. The induction of cell cycle regulatory and DNA repair proteins in cisplatin-induced acute renal failure. Toxicol Appl Pharmacol. 2004;200:111–20.
18 Uchino S, Kellum JA, Bellomo R, Doig GS, Morimatsu H, Morgera S, et al. Acute renal failure in critically ill patients: a multinational, multicenter study. JAMA. 2005;294:813–8.
19 Imasawa T, Utsunomiya Y, Kawamura T, Zhong Y, Nagasawa R, Okabe M, et al. The potential of bone marrow-derived cells to differentiate to glomerular mesangial cells. J Am Soc Nephrol. 2001;12:1401–9.
20 Morigi M, Imberti B, Zoja C, Corna D, Tomasoni S, Abbate M, et al. Mesenchymal stem cells are renotropic, helping to repair the kidney and improve function in acute renal failure. J Am Soc Nephrol. 2004; 15:1794–804.
21 Lange C, Togel F, Ittrich H, Clayton F, Nolte-Ernsting C, Zander AR, et al. Administered mesenchymal stem cells enhance recovery from ischemia/reperfusion–induced acute renal failure in rats. Kindney Int. 2005;68:1613–7.
22 Hung SC, Deng WP, Yang WK, Liu RS, Lee CC, Su TC, et al. Mesenchymal stem cell targeting of microscopic tumors and tumor stroma development monitored by noninvasive in vivo positron emission tomography imaging. Clin Cancer Res. 2005;11:7749–56.
23 Shichinohe H, Kuroda S, Lee JB, Nishimura G, Yano S, Seki T, et al. In vivo tracking of bone marrow stromal cells transplanted into mice cerebral infarct by fluorescence optical imaging. Brain Res Brain Res Protoc. 2004;13:166–75.
24 Weissleder R. Molecular imaging: exploring the next frontier. Radiology. 1999;212:609–14.
25 Daldrup-Link HE, Rudelius M, Oostendorp RA, Settles M, Piontek G, Metz S, et al. Targeting of hematopoietic progenitor cells with MR contrast agents. Radiology. 2003;228:760–7.
26 Weissleder R, Stark DD, Engelstad BL, Bacon BR, Compton CC, White DL, et al. Superparamagetic iron oxide: pharmacokinetics and toxicity. AJR. 1989;152:167–73.

Established in 1871

Formerly: Schweizerische Medizinische Wochenschrift

SMW Swiss Medical Weekly

The European Journal of Medical Sciences

The many reasons why you should choose SMW to publish your research

What Swiss Medical Weekly has to offer:

- SMW's impact factor has been steadily rising. The 2006 impact factor is 1.346.
- Open access to the publication via the Internet, therefore wide audience and impact
- Rapid listing in Medline
- LinkOut-button from PubMed with link to the full text website http://www.smw.ch (direct link from each SMW record in PubMed)

- No-nonsense submission – you submit a single copy of your manuscript by e-mail attachment
- Peer review based on a broad spectrum of international academic referees
- Assistance of professional statisticians for every article with statistical analyses

- Fast peer review, by e-mail exchange with the referees
- Prompt decisions based on weekly conferences of the Editorial Board
- Prompt notification on the status of your manuscript by e-mail
- Professional English copy editing

We evaluate manuscripts of broad clinical interest from all specialities, including experimental medicine and clinical investigation.

We look forward to receiving your paper!

Guidelines for authors:
http://www.smw.ch/set_authors.html

All manuscripts should be sent in electronic form, to:

EMH Swiss Medical Publishers Ltd.
SMW Editorial Secretariat
Farnsburgerstrasse 8
CH-4132 Muttenz

Manuscripts:	submission@smw.ch
Letters to the editor:	letters@smw.ch
Editorial Board:	red@smw.ch
Internet:	http://www.smw.ch

EMH FMH Schwabe
Editores Medicorum Helveticorum

Official journal of the Swiss Society of Infectious Diseases, the Swiss Society of Internal Medicine and the Swiss Respiratory Society

Supported by the FMH (Swiss Medical Association) and by Schwabe AG, the long-established scientific publishing house founded in 1488